Ionics (2022) 28:4697–4708
https://doi.org/10.1007/s11581-022-04687-0

ORIGINAL PAPER

One-pot electro-co-deposition of nanospherical polydiphenylamine-palladium–supported graphitic carbon nitride nanohybrid for efficient methanol oxidation

Suba Lakshmi Madaswamy[1] · K. Vengadesan[1,2] · Saikh Mohammad Wabaidur[3] · Md Ataul Islam[4] · Muthukrishnan Francklin Philips[5] · Vasudevan Dhayalan[1] · Ragupathy Dhanusuraman[1]

Received: 28 April 2022 / Revised: 14 July 2022 / Accepted: 15 July 2022 / Published online: 25 August 2022

Abstract

In this work, a novel co-deposited nano spherical polydiphenylamine-palladium supported graphitic carbon nitride (GCN/PDPA/Pd NS) nanohybrid was fabricated via the in-situ one-pot electrochemical co-deposition method. The GCN/PDPA/Pd NS nanohybrid electrode was characterized by morphology studies, which found that the average diameter of the PDPA/Pd nanospherical size is 250 nm over the graphitic carbon nitride nano matrix as well as elemental composition, structural and vibrational spectra also observed through FESEM, EDX, Mapping, and XRD, FT-IR studies. The electrochemical characterizations of the GCN/PDPA/Pd NS electrocatalyst were studied using cyclic voltammetry, chronoamperometry, and electrochemical impedance spectroscopic techniques. The fabricated GCN/PDPA/Pd NS–modified electrode shows significant electrocatalytic activity, lower oxidation potential (− 0.15 V), high stability, and longevity (1800s) towards methanol oxidation reaction (MOR) in an alkaline medium. The fabricated GCN/PDPA/Pd NS electrocatalyst is a significant anode catalyst for the direct methanol fuel cell application.

Keywords Electrochemical method · GCN/PDPA/Pd nanospherical · Methanol oxidation reaction · DMFC

Introduction

Direct methanol fuel cell (DMFC) is one of the greatest ecologically sustainable and exciting sources of electricity for upcoming developments to be used in portable energy sources, electric vehicles, and transport applications [1, 2], for the reason that DMFC has outstanding properties such as high energy density, high-power proficiency, least possible emission, cost-effectiveness, ambient operation state, safety operation, and easy storage. A DMFC has been viewed as a very promising power source device for the future due to its unique merits, which include its theoretically high conversion efficiency (more than 96%), liquid methanol fuel handling safety compared to that of hydrogen, and nearly zero pollution emission [3]. Platinum (Pt) is the most effective and most widely used electrocatalyst for methanol oxidation reaction (MOR) in DMFCs. However, platinum-based catalysts struggle with several difficulties such as expensive, insufficient stability, rare availability of Pt, combined with the catalyst poisoning impact caused by methanol oxidation reaction products (carbon monoxide (CO)) on the Pt catalyst, needed a search for alternative catalytic systems. So, these problems are overcome by one of the most potential candidates to substitute platinum which is palladium (Pd), which has been extensively studied as an efficient anode catalyst for fuel cell reactions [4, 5].

Therefore, the growth of highly active Pd-based anode catalysts has attracted considerable attention as a promising

✉ Ragupathy Dhanusuraman
ragu.nitpy@gmail.com; ragu@nitpy.ac.in

1 Nano Electrochemistry Lab (NEL), Department of Chemistry, National Institute of Technology Puducherry, Karaikal 609609, India

2 Department of Chemistry, St. Joseph's College of Arts and Science (Autonomous), Cuddalore, Tamil Nadu, India

3 Chemistry Department, College of Science, King Saud University, Riyadh 11451, Saudi Arabia

4 Division of Pharmacy and Optometry, School of Health Science, Faculty of Biology, Medicine and Health, University of Manchester, Manchester, UK

5 P.G. and Research Department of Chemistry, Bishop Heber College (Autonomous), Tamil Nadu, Tiruchirappalli 620017, India

electrocatalyst for MOR owing to their higher surface area, superior electrocatalytic activity superior resistance to the formation of CO-like intermediates in an alkaline medium, and inexpensive compared to Pt-based electrocatalysts. The catalytic activity of pure Pd catalyst can be improved by (1) conducting polymers such as polyaniline, polydiphenylamine, and polypyrrole, and (2) carbon-based materials such as graphene, carbon nanotube, and graphitic carbon nitride [6–11]. Palladium-based catalysts have emerged as a good electrode material for oxidation in an alkaline medium.

Among the conducting polymers, polyaniline (PANI) and its derivatives, such as poly(2,5-dimethoxyaniline) (PDMA) and polydiphenylamine (PDPA) have fascinating properties like solubility, high conductivity, reversible redox behavior, significant electrochemical stability, reasonable price, and eco-friendly and hybrid permutations in diverse application spreads to electrocatalytic activity, biosensor, supercapacitor, and electrocatalytic oxidation [12–21]. The conducting polymer of polydiphenylamine is an N-substituted form of polyaniline and it has some special properties such as being highly soluble in organic solvents, excellent electrocatalytic activity, and particularly it has two stable oxidized forms, polaronic (diphenylbenzidine cation, $DPSI^{+}$) and bipolaronic (diphenylbenzidine dication, $DPSI^{2+}$) structures [22, 23]. Also, the conducting polymer of PDPA enhances the electrocatalytic activity of palladium metal nanoparticles. Along carbon-based material also boosts electrocatalytic activity and stability because of its vastly admirable electrical conductivity, virtuous stability, and low-price. Among the material, graphitic carbon nitride (GCN) is a 2-dimensional arrangement like graphite material which can be regarded as N-substituted graphite and a potential source of free-standing nitrogen-rich carbon material. The (GCN) has enhanced the electrocatalytic activities because of its exclusive properties, like greater surface area, high porosity, ultrahigh nitrogen content, unique electronic and optical properties, and, inexpensive which has been used in various applications such as photocatalyst, fuel cells, supercapacitor, and sensors [17, 24–30]. Based on several studies that have focused on reducing the Pt loading or alternating metals such as palladium (Pd), nickel (Ni), (cobalt), iron (Fe), etc., and carbon-based materials such as graphene, graphitic carbon nitride, and conducting polymers such a polyaniline and their derivatives were used [31–38]. Considering literature reviews, the nanocomposites of polydiphenylamine-palladium supported graphitic carbon nitride exposed to enhance the electro-catalytic properties, and also simple method, better stability, durability, and low-priced towards methanol oxidation reaction.

Here, we fabricate a single-step process of a novel co-deposited nano spherical polydiphenylamine-palladium–supported graphitic carbon nitride nano spherical composite (GCN/PDPA/Pd NS) as an anode electrocatalyst for the methanol oxidation reaction. The resulting GCN/PDPA/Pd NS–modified electrode has been characterized by field-emission scanning electron microscopy (FESEM) with energy-dispersive X-ray spectroscopy (EDX) and mapping analysis, Fourier-transform infrared (FT-IR), and X-ray diffraction (XRD) methods. The electrochemical activity of the modified electrode was studied via cyclic voltammetry (CV), impedance spectroscopy (EIS), and chronoamperometry (CA) methods. The fabricated modified (GCN/PDPA/Pd NS) electrode delivers enhanced electro-catalytic performance for the electro-oxidation reaction of methanol with high stability and longevity.

Experimental

Chemicals

All the chemicals such as diphenylamine (DPA), melamine, and palladium (Pd), were purchased from Merck India. A FTO-coated glass substrate (25 mm × 25 mm × 1.1 mm, resistivity < 10 Ω) was purchased from Sigma-Aldrich. The distilled water was only used for this full experiment.

Reagents

The reagents of sulfuric acid (H_2SO_4), potassium hydroxide (KOH), and methanol were purchased from Merck India.

Instrumentations

The structural information and elemental examination of the modified electrode were derived from FESEM (Tescan-Mira 3-LMH) with EDX and mapping (Bruker Quantax 200). The study of the crystalline nature of the material was carried out by powder XRD pattern using the Rigaku Smart Lab X-ray diffractometer equipped with CuKα radiation. Vibrational spectra of the samples were observed by Perkin Elmer making Model Spectrum RX1 (Range 4000–400 cm^{-1}) using the KBr compressed pellet method. All the electrochemical measurements of CV, CA, and EIS techniques were performed using an electrochemical workstation (OrigaLys-OFG500, France). In this FTO-modified electrode, platinum, and calomel were used as a working electrode, a counter electrode, and a reference electrode, respectively.

Preparation of GCN/PDPA/Pd modified nanohybrid electrode

Synthesis of graphitic carbon nitride (GCN)

Graphitic carbon nitride (GCN) was synthesized by the pyrolysis method. The precursor of melamine powder (5 g)

was taken into the alumina crucible. Then, crucible was put in a muffle furnace, which was maintained at up to 500° C under an argon atmosphere. After the reaction, crucible was cooled at room temperature. Finally, a pale-yellow fine powder was obtained [31].

Fabrication of modified GCN/PDPA/Pd nanohybrid electrode

In this fabrication of modified GCN/PDPA/Pd nanohybrid electrode by the in situ one-pot electrochemical co-deposition method, the precursor of 40 mM diphenylamine, 0.5 g of GCN, and 0.01 M $PdCl_2$ (3:3:1 ratio) were dissolved in 0.5 M H_2SO_4, which was well stirred up to 30 min in order to obtain a milky yellow color homogenous mixture solution. Then, FTO substrate was immersed into the above resultant mixture and applied potential ranging from − 0.1 to 1 V at a scan rate of 100 mV/s for 10 cycles. Finally, GCN/PDPA/Pd NS nanohybrid was electro co-deposited onto the FTO substrate and then dried under ambient temperature overnight. The overall schematic illustration of GCN/PDPA/Pd NS nanohybrid towards MOR is shown in Fig. 1.

Results and discussion

Morphology and elemental analysis

The morphology of (A) GCN, (B) PDPA and (C–E) GCN/PDPA/Pd NS nanohybrid electrode was shown in Fig. 2. Figure 2A GCN depicts the irregular sheet like structure, and Fig. 2B PDPA shows the beads like granules morphology. The shape and surface morphology of the lower and higher magnification of the modified GCN/PDPA/Pd NS nanohybrid electrode were shown in Fig. 2C–E. The co-deposited GCN/PDPA/Pd NS nanocomposite morphology shows the nano spherical structure PDPA/Pd over the graphitic carbon nitride nano matrix background (Fig. 2A and B). The average nano spherical size of PDPA/Pd is around 250 nm, which was revealed in Fig. 2C. This nano spherical PDPA/Pd is attached to the surface of the graphitic carbon nitride nano matrix due to the electrostatic interaction. It is clear that nano spherical PDPA/Pd is homogeneously distributed on the surface of the graphitic carbon nitride matrix. Graphitic carbon nitride matrix is used as support material for deposition of PDPA and Pd particles, such structure would be advantageous of additional point to improve the electroactivity of the nanocomposite. The chemical composition and elemental mapping analysis were done by Energy dispersive X-ray (EDX) spectroscope attached to the FESEM and the corresponding elemental map is existing in Fig. 3A and B. The EDX spectra with mapping analysis designate the existence of elements in the GCN/PDPA/Pd NS nanohybrid electrodes such as carbon (Fig. 3C), nitrogen (Fig. 3D), oxygen (Fig. 3E), and palladium (Fig. 5F) were exhibited, individually.

Crystallographic

The XRD study was performed to determine the type of the synthesized material (crystalline or amorphous) and the size of the particles. The fabricated GCN, PDPA,

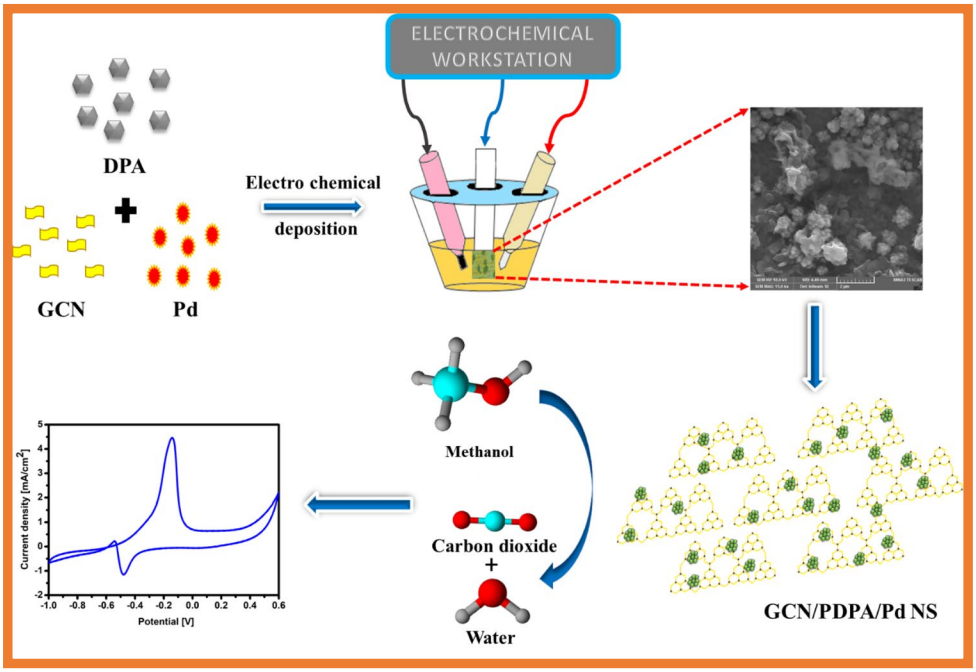

Fig. 1 The overall schematic illustration of GCN/PDPA/Pd NS nanohybrid towards MOR

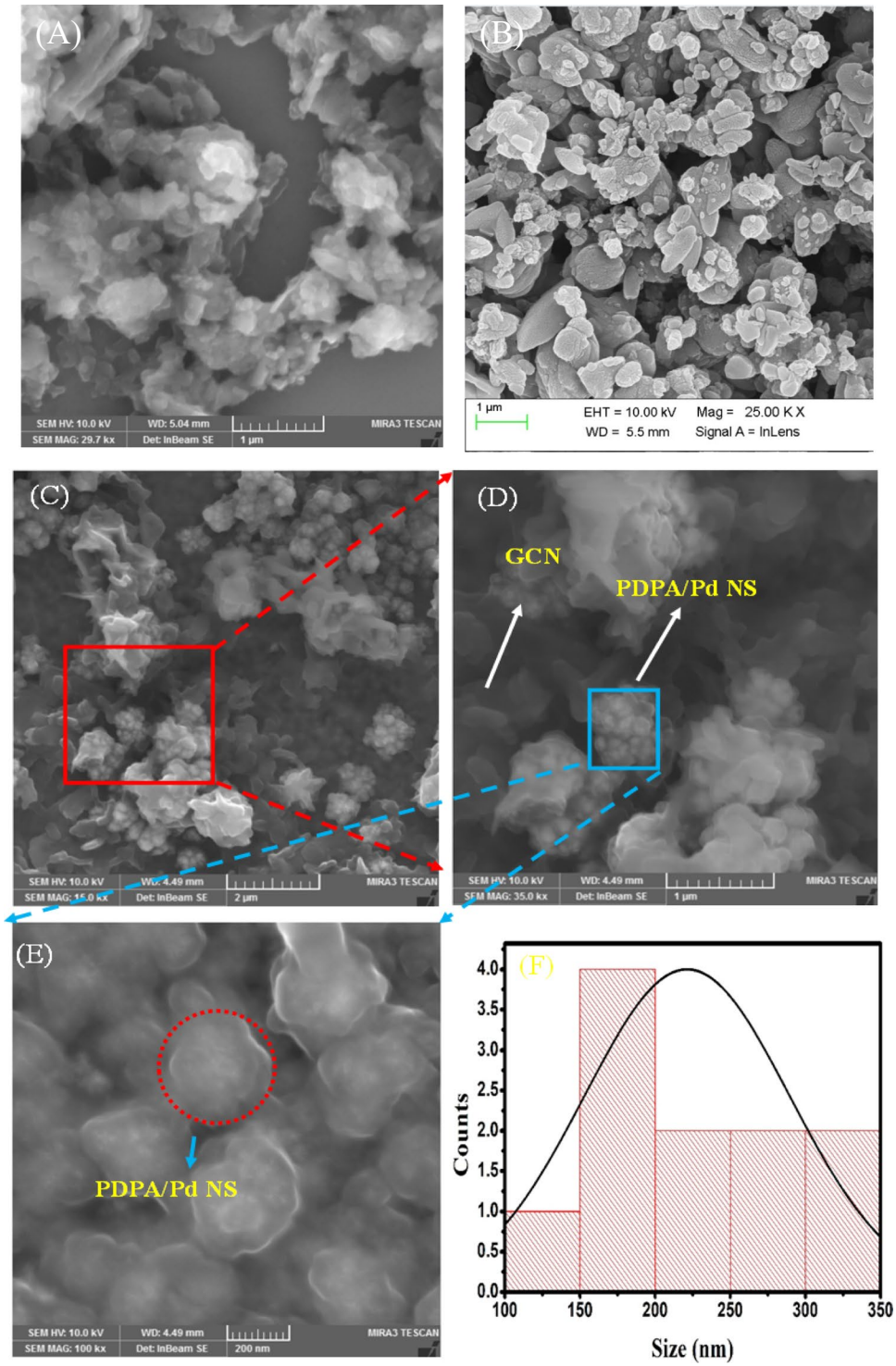

Fig. 2 FESEM images of (**A**) GCN, (**B**) PDPA, (**C**) GCN/PDPA/Pd NS nanohybrid, (**D**) magnified image of (**C**), (**E**) magnified image of (**D**), and (**F**) Particle size distribution curve obtained from SEM images (**E**)

GCN/PDPA/Pd NS nanohybrid electrode XRD pattern was revealed in Fig. 4. The Miller reflections of (100) and (002) are shown by the strong peaks of GCN in Fig. 4a at 2 θ = 12° and 27.5°, respectively. Figure 4b PDPA has distinctive sharp peaks in diffraction at 18.5° and Fig. 4c GCN/PDPA/Pd NS nanohybrid shows the characteristic peaks such as 2θ = 12°, 26.5°, 40.2°, 46.5°, 68° representatives of the Miller reflections of (100), (002), (111), (200), (220), correspondingly. The distinguishing diffraction peaks positioned at 2 θ values are well-matched with the standard diffraction pattern of Pd (JCPDS-89–4897), which confirms the presence of Pd in the GCN/PDPA. Additionally, the diffraction peaks position at 2θ = 40.2°, 46.5°, 68° consistent with the (1 1 1),

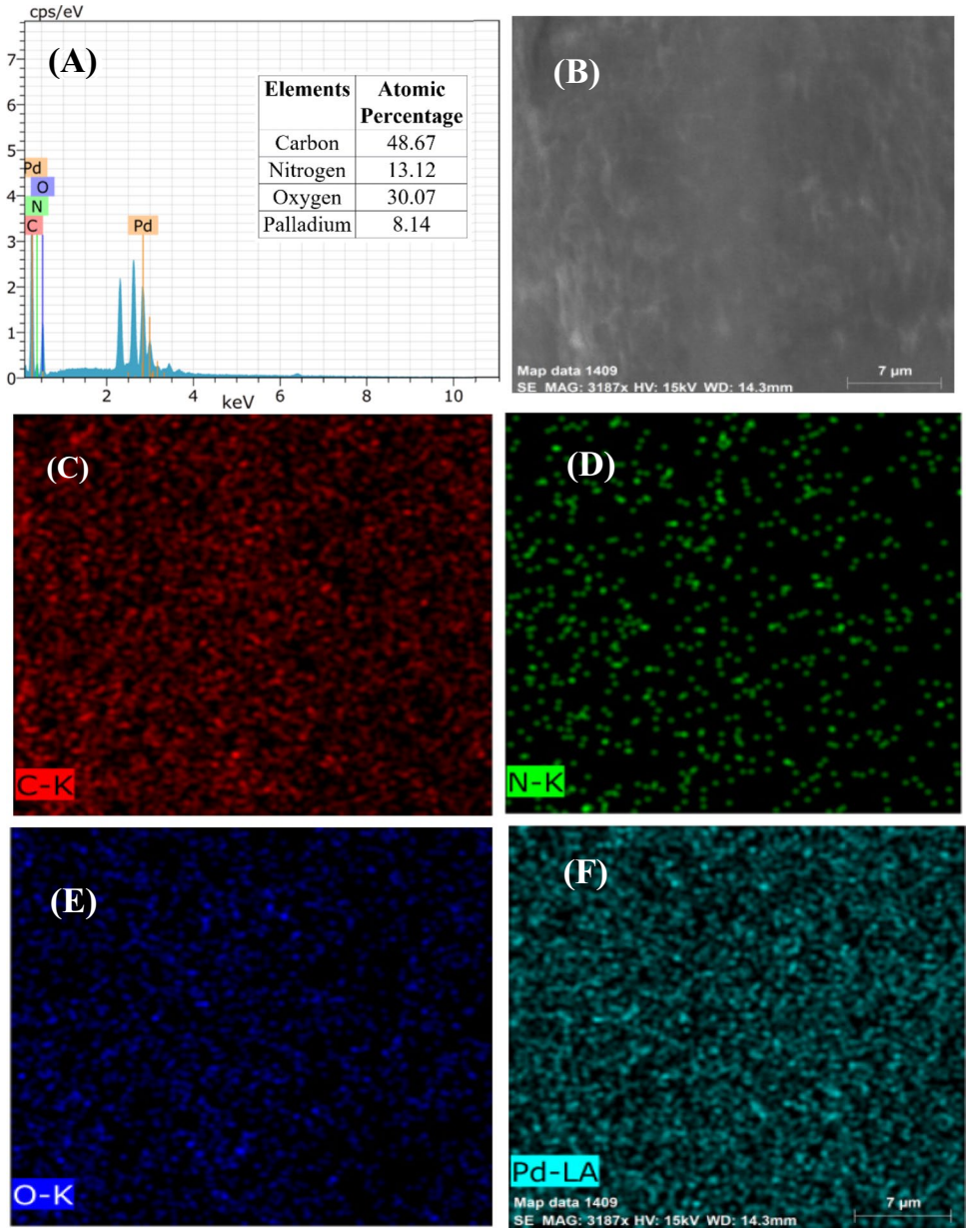

Fig. 3 **A** EDX and (**B**) FESEM with mapping Image (**C**–**F**) of GCN/PDPA/Pd NS nanohybrid

(2 0 0) and (2 2 0) index planes in the face-centered cubic (fcc) structure of Pd and the peak at 12° (100), 26.5° (0 0 2) was attributed to graphitic carbon nitride (12° (100), 26.5° (0 0 2)) and PDPA (26.5° (0 0 2)), respectively [6, 11, 32], some of the peaks are shifted due to the synergistic behaviour and π-π interactions, which are caused by the hybrid formation of GCN, PDPA, and Pd nanoparticles. The size of the Pd nanostructure was derived from Pd (1 1 1) peak and found to be about 9.98 nm by the Debye–Scherrer equation. These nanostructures of Pd are responsible for the electrocatalytic activity of the nanocomposite.

Structural analysis

FTIR analysis was carried out to confirm the interaction of composite. Figure 5 shows the vibration spectra of the GCN, PDPA, GCN/PDPA/Pd NS nanohybrid electrode within the range of 4000 to 500 cm^{-1}. Figure 6a Due to the amine group's amine stretching frequency, GCN exhibits a large peak at 3310 cm^{-1}. The C = N stretching modes are thought to be responsible for the strong bands at 1671 and 1437 cm^{-1}, the band at 1100 cm^{-1} to the vibration of the C-N stretching, this corresponds to the characteristic IR signature of aromatic amines, and the band at 840 cm^{-1},

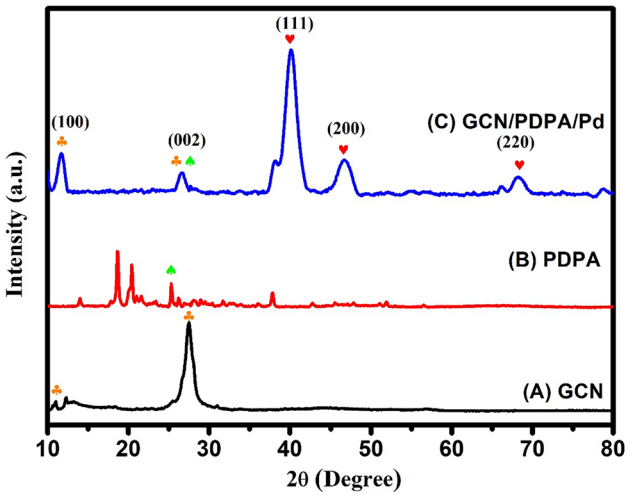

Fig. 4 XRD spectrum of (**A**) GCN, (**B**) PDPA, (**C**) GCN/PDPA/Pd NS nanohybrid

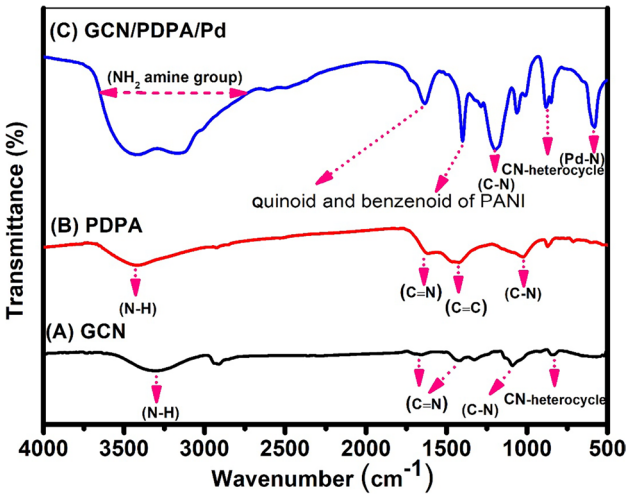

Fig. 5 FT-IR spectrum of (**A**) GCN, (**B**) PDPA, (**C**) GCN/PDPA/Pd NS nanohybrid

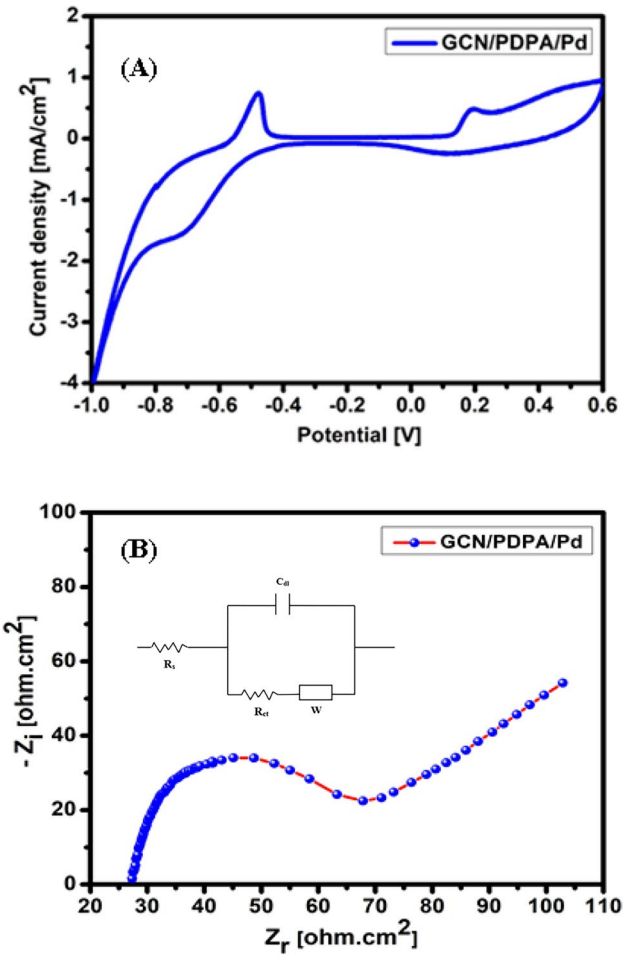

Fig. 6 (**A**) Cyclic voltammetry curves of GCN/PDPA/Pd in 0.5 M H_2SO_4 at scan rate of 100 mV s^{-1} and (**B**) Nyquist plot of EIS for GCN/PDPA/Pd in 0.5 M H_2SO_4

which corresponds to the S-triazine rings' out-of-plane bending vibration frequency. These findings demonstrate that GCN was successfully synthesized. Figure 6b PDPA has a peak at 3301 cm^{-1} that is linked to N–H bond stretching vibration mode, the C = N and C = C stretching in quinoid and benzenoid phenyl rings are characterized by the high characteristic peaks at 1419 and 1318 cm^{-1}, respectively. The peak at 1090 cm^{-1} is attributed to the C-N modes of the secondary aromatic amine, while the peak at 805 cm^{-1} is attributed to the out-of-plane bending of aromatic C-H, respectively. Figure 6c depicts GCN/PDPA/Pd NS nanohybrid. From the spectra, the range of 3600–3000 cm^{-1} shows the peaks that indicate the primary and secondary amines of N–H stretching frequency. The sharp characteristic peaks at 1625 and 1402 for C = N and C = C of quinonoid and benzenoid structures of PDPA, correspondingly. A strong sign at 1210 cm^{-1} is characteristic of the C-N stretching vibration which is the universal representative IR sign of the aromatic amines. The intense band at 847 cm^{-1} characterized the out-of-plane bending vibration frequency of the S-triazine unit. Moreover, the intense peak at 578 cm^{-1} is a significant characteristic peak of the Pd–N bond [6, 11, 17, 19]. These FTIR outcomes confirm the interaction of GCN/PDPA/Pd NS nanohybrid.

Electrochemical characterizations of modified GCN/PDPA/Pd NS nanohybrid electrode

Cyclic voltammetry catalytic activity of modified GCN/PDPA/Pd NS nanohybrid electrode

CV performances of modified GCN/PDPA/Pd NS nanohybrid electrode electrocatalytic activity are revealed in

Fig. 6(A). CV peaks of modified GCN/PDPA/Pd NS nanohybrid electrode showed a pair of redox forms in the potential range amid − 1.0 V and 0.6 V at a scan rate of 100 mV/s in 0.5 M H_2SO_4 medium. The first redox peak appeared at − 0.48/ − 0.71 V, which displays the oxidation and reduction form of the adsorbed and absorbed hydrogen (H_{ad} and H_{ab}), and the second redox peak seemed at 0.2/0.1 V confirms the transformation of the polaronic structure of PDPA to the bi-polaronic structure of diphenoquinone diamine ($DPDI^{2+}$) [14]. These peaks proved the electrodeposition of GCN/PDPA/ Pd nanohybrid on the FTO substrate.

Electrochemical impedance spectroscopy

Electrochemical impedance is an important approach to analyzing the charge transfer resistances of the modified electrode. Figure 6(B) shows the impedance behavior of fabricated modified GCN/PDPA/Pd NS nanohybrid electrode in 0.5 M H_2SO_4 medium. This Nyquist plot attained a small semicircle in the high-frequency region and also a straight sloppy line in the lower-frequency region. The charge-transfer resistance (Rct) of GCN/PDPA/Pd NS nanohybrid showed a value of 40 Ω. Thus, the smaller semicircle reveals the lower charge transfer resistance (R_{ct}) which shows that the faster reaction rate of modified GCN/PDPA/Pd NS nanohybrid electrodes is due to the synergistic interaction of the nanohybrid.

The electrocatalyst's electrochemical behavior was investigated in a typical ferrocyanide/ferricyanide solution with 5 mM $K_3Fe(CN)_6$ and $K_4Fe(CN)_6$ diluted in 0.1 M KCl serving as the supporting electrolyte. The findings of CV in the range of 0.2 to + 0.8 V are shown in Fig. 7(A). The outcomes demonstrate the electrode's strong faradaic reaction to the ferro/ferri couple's electron transport. Using the Randles–Sevcik equation, electrochemical surface area (ECSA), a crucial electro-catalyst parameter, has been determined. $Ip = 2.69 \times 10^5 \times A \times D^{1/2} \times n^{2/3} \times \upsilon^{1/2} \times C$ is the scan rate of the potential perturbation (0.05 V s^{-1}), Ip is the redox peak current, A is the area of the electroactive surface area (cm^2), D is the diffusion coefficient of the molecule in solution (cm^2), n is the number of electrons participating in the redox reaction (n = 1), and C is the bulk concentration of the redox probe (5 Mm) [21]. The ECSA of commercial Pd/C catalyst and GCN/PDPA/Pd NS nanohybrid electrodes is 11.68 cm^2 and 86.96 cm^2, GCN/PDPA/Pd NS electrocatalyst has a greater ECSA than commercial Pd/C, electrocatalyst, which is depicted in Table 1.

Electrocatalytic activity towards MOR

The electrocatalytic properties of the GCN/PDPA/Pd NS nanohybrid toward methanol oxidation in an alkaline medium were assessed in detail. A commercial Pd/C catalyst is used as a benchmark material for comparison. Figure 7(B) shows the CV studies of the commercial Pd/C catalyst and GCN/PDPA/Pd NS nanohybrid in a solution containing 0.5 M KOH by the potential range amid − 1.0 V and 0.6 V at a scan rate of 100 mV/s. Figure 7(C) analyzes the CV studies of commercial Pd/C catalyst and GCN/PDPA/Pd NS nanohybrid in 0.5 M KOH and 1 M methanol medium by the potential range amid − 1.0 V and 0.6 V at a scan rate of 100 mV/s, carried out to evaluate the catalytic activity towards methanol oxidation, which displays a pair of oxidation peak at − 0.15/ − 0.54 V in forward and backward scans, which is much lower than the onset voltage and for commercial Pd/C (− 0.057/ − 0.47 V), as well as the current densities of the GCN/PDPA/Pd NS nanohybrid, is 4.5 mA/cm^2 for forwarding scan peak and 0.2 mA/cm^2 reverse scan oxidation peak, which is comparatively 3 times higher than the commercial Pd/C catalyst current densities. The negative shift (0.093 V) of the oxidation potential specifies the improved electrocatalytic activity of the nanocomposite. In this, the first anodic peak in the forward scan is due to the oxidation of chemisorbed intermediate like carbonaceous species CO from methanol adsorption on the façade of the electrocatalyst and another anodic peak in the backward scan can be due to the oxidation of CO to CO_2, which easily desorbed from the surface of the catalyst [11]. Electrochemical characteristics of the proposed modified GCN/PDPA/Pd NS nanohybrid electrode significantly lower oxidation potential and higher current density than other reported electrocatalysts [12, 17,] which is shown in Table 2. The superior electrocatalytic activity of the modified GCN/PDPA/Pd NS nanohybrid electrode is the synergistic interaction of the GCN, PDPA, and Pd materials as well as the nano spherical morphology of palladium nanostructure.

Figure 8 shows the effect of potential sweep rates on GCN/PDPA/Pd NS nanohybrid electrodes at different scan rates from 5 to 100 mV s^{-1} in 0.5 M KOH and 1 M MeOH (Fig. 8A). The current densities of the forward and backward scan rising by increasing scan rate as well as a positive shift in the forward peak potential and a negative shift in the backward peak potential. These shifts of a couple of well-defined peaks suggested that the reaction process was regulated by irreversible oxidation. Besides, the cathodic peak at negative potentials in the backward scan indicated

Table 1 The anodic peak current and the electroactive surface area of modified electrodes

No	Modified electrodes	Anodic peak current (A)	Electrochemical active surface area (cm^2)
1	(a) Pd/C	0.0024	11.68
2	(b) GCN/PDPA/ Pd NS	0.0157	86.96

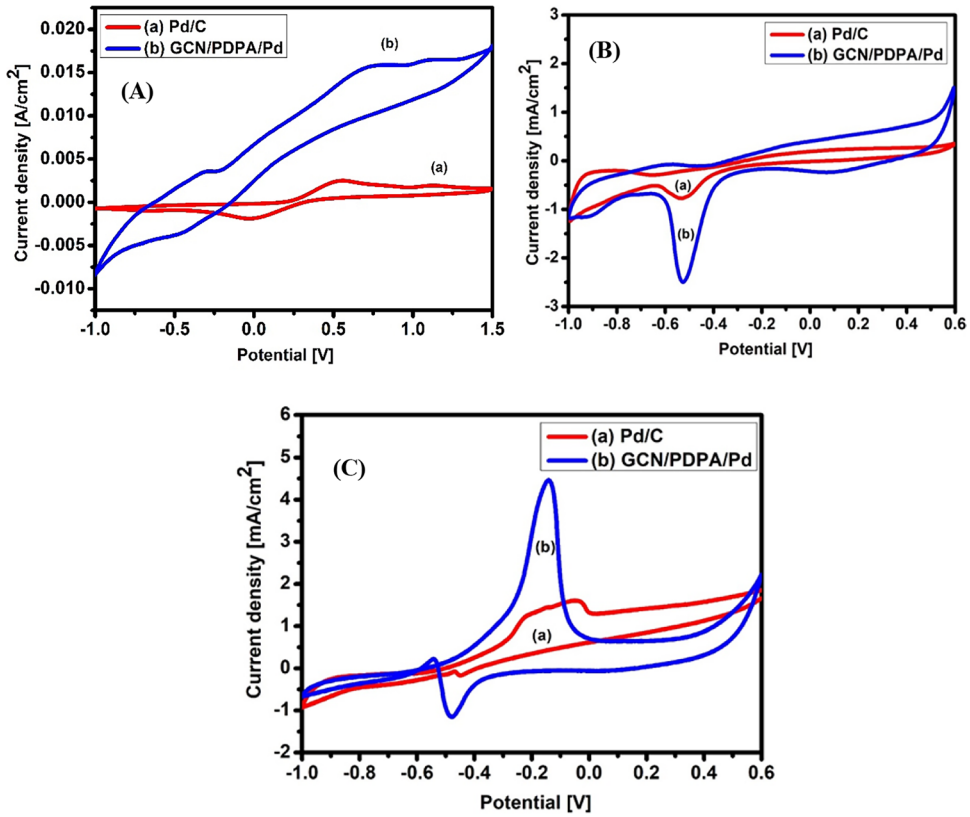

Fig. 7 Cyclic voltammetry curves in (**A**) (a) Pd/C and (b) GCN/ PDPA/Pd in 0.1 M KCl containing 5 mM $Fe(CN)_6^{-3/-4}$ at the scan rate of 50 mV/s (**B**) (a) Pd/C and (b) GCN/ PDPA/Pd in 0.5 M KOH absence of methanol (**C**) (a) Pd/C and (b) GCN/ PDPA/Pd 0.5 M KOH presence of 1M methanol at scan rate of 100 mV s^{-1}

Table 2 Comparison of electrochemical performance of Pd based catalyst towards MOR

S no	Electrocatalyst	Potential window	Methanol oxidation conditions	Oxidation potential	Ref no
1	Pd/PANI/TiO_2/GC	− 0.8 to 0.5 V	1 M Methanol in 0.5 M KOH	− 0.1 mV	[12]
2	g-C_3N_4/PANI/Pd	− 0.6 to 0.6 V	1 M Methanol in 0.5 M KOH	0.24 V	[17]
3	GCN/PDPA/Pd NS	− 1.0 to 0.6 V	1 M Methanol in 0.5 M KOH	− 0.15 mV	This work

that the oxidation of methanol and the desorption of the intermediates formed entirely. Figure 8B depicts the Plot of scan rate vs. forward peak current density of Fig. 8A. This experiment indicates the diffusion process of GCN/ PDPA/Pd NS nanohybrid electrocatalytic activity in methanol oxidation reaction in alkaline solution [11].

Figure 8C displays the influence of different methanol concentrations on the GCN/PDPA/Pd NS nanohybrid electrode electro-catalytic activity towards MOR. The methanol concentration from 1 to 7 M grows up, the current density of the oxidation peak also increases and the potential also shifted forward which shows in Fig. 8C. Figure 8D illustrates the plot of concentration vs. forward peak current density of Fig. 8C. The peak potential shifts to the positive potential because of the active sites at the electrode's surface and the direct correlation between the overpotential of methanol oxidation reaction (IR drop) and the amount of oxidation current [11].

Stability of the modified GCN/PDPA/Pd NS nanohybrid electrode for MOR

The electrocatalyst stability is an important factor for their practical application in DMFCs. The cyclic voltammetry and chronoamperometric studies revealed the long-term stability of the fabricated modified GCN/PDPA/Pd NS nanohybrid electrode in Fig. 9. Figure 9A reveals the stability of GCN/PDPA/Pd NS nanohybrid electrode was swept potential window between − 0.1 and 0.6 V in a solution of 0.5 M KOH and 1 M methanol for 50 cycles with the scan rate of 100 mV s^{-1}. The current densities of the GCN/PDPA/Pd NS nanohybrid were constant with increasing cycle numbers (1st

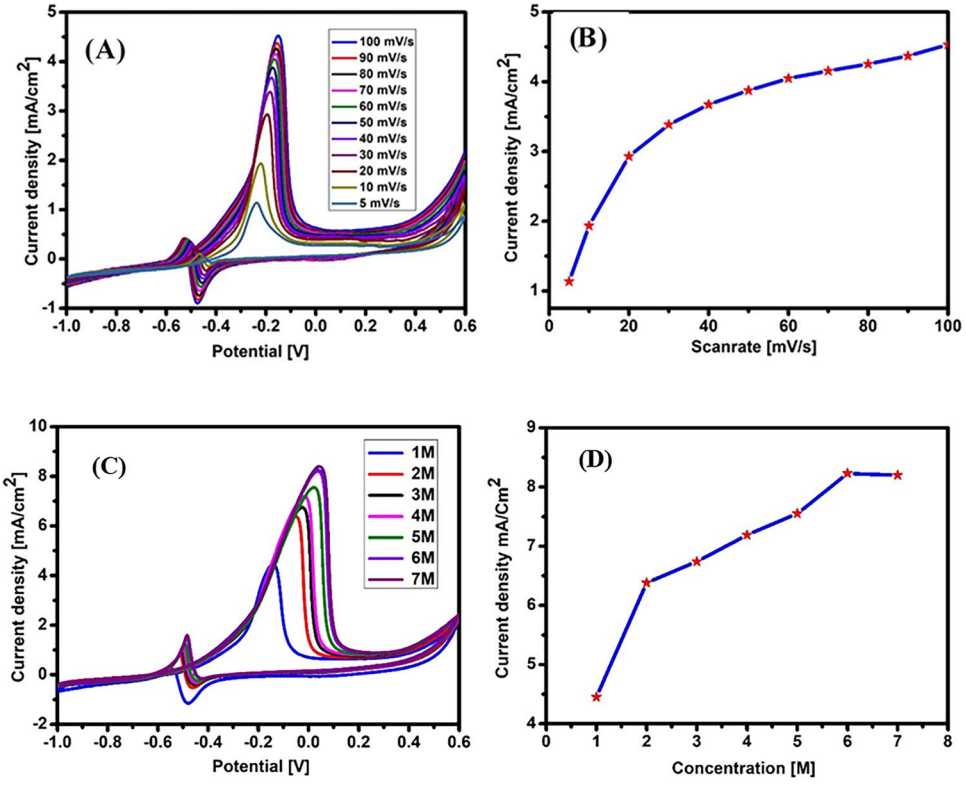

Fig. 8 Cyclic voltammetry curves in (**A**) (a) GCN/PDPA/Pd in 0.5 M KOH of 1 M methanol at different scan rate (5–100 mV s^{-1}), (**B**) Plot of scan rate vs. peak current density of (**A**), (**C**) Cyclic voltammetry curves of GCN/PDPA/Pd in 0.5 M KOH of 1 M methanol at different concentration (1–7 M), and (**D**) Plot of concentration vs. peak current density of (**C**)

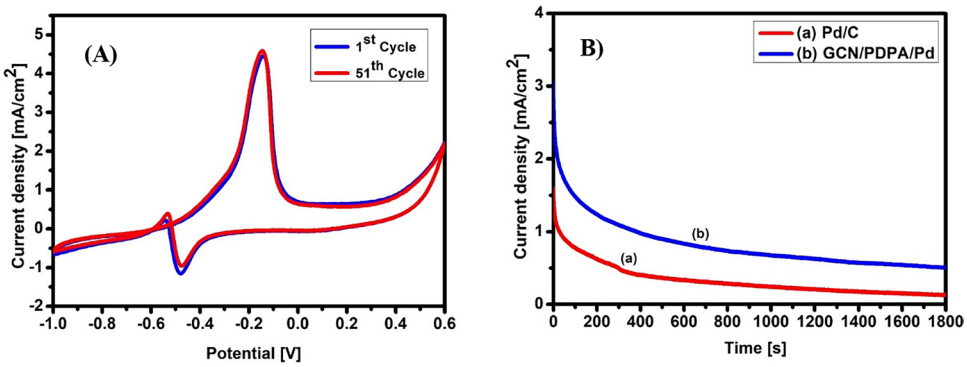

Fig. 9 CV curves of (**A**) Stability of GCN/PDPA/Pd in 0.5 M KOH of 1 M methanol and (**B**) Chronoamperometric curves 1 M CH_3OH with a scan rate of 100 mV s^{-1} at − 0.15 V at room temperature in 0.5 M KOH

cycle to 50th cycle), which proves that GCN/PDPA/Pd NS nanohybrid electrodes have long-term stability and strong electrocatalytic activity toward MOR Fig. 10.

The CA studies were carried out to investigate the stability and durability of the commercial Pd/C catalyst and modified GCN/PDPA/Pd NS nanohybrid electrode in 0.5 M KOH and 1.0 M methanol at − 0.15 V during the 1800s was shown in Fig. 9B. Figure 9B (a) commercial Pd/C catalyst shows the initial current density of 1.4 mA/cm^2, which slowly decreased to 0.13 mA/cm^2 after the 1800s, and Fig. 9B (b) displays the initial current density of 3.1 mA/cm^2, which slowly decreased to 0.5 mA/cm^2 after 1800s. These results prove that GCN/PDPA/Pd NS nanohybrid electrode exhibited less decay current than the commercial Pd/C catalyst. The synergistic interactions of GCN/PDPA/Pd NS nanohybrid and their mechanism of has shown in Fig. 10 (A & B). The GCN/PDPA/Pd NS nanohybrid electrode has higher stability and better poisoning tolerance ability towards methanol oxidation.

Conclusion

In this study, a novel GCN/PDPA/Pd NS nanohybrid electrode was fabricated by an in situ one-pot electrochemical co-deposition method. The GCN/PDPA/Pd NS nanohybrid electrode morphology and the structural features were investigated by FE-SEM, FTIR, and XRD characterization.

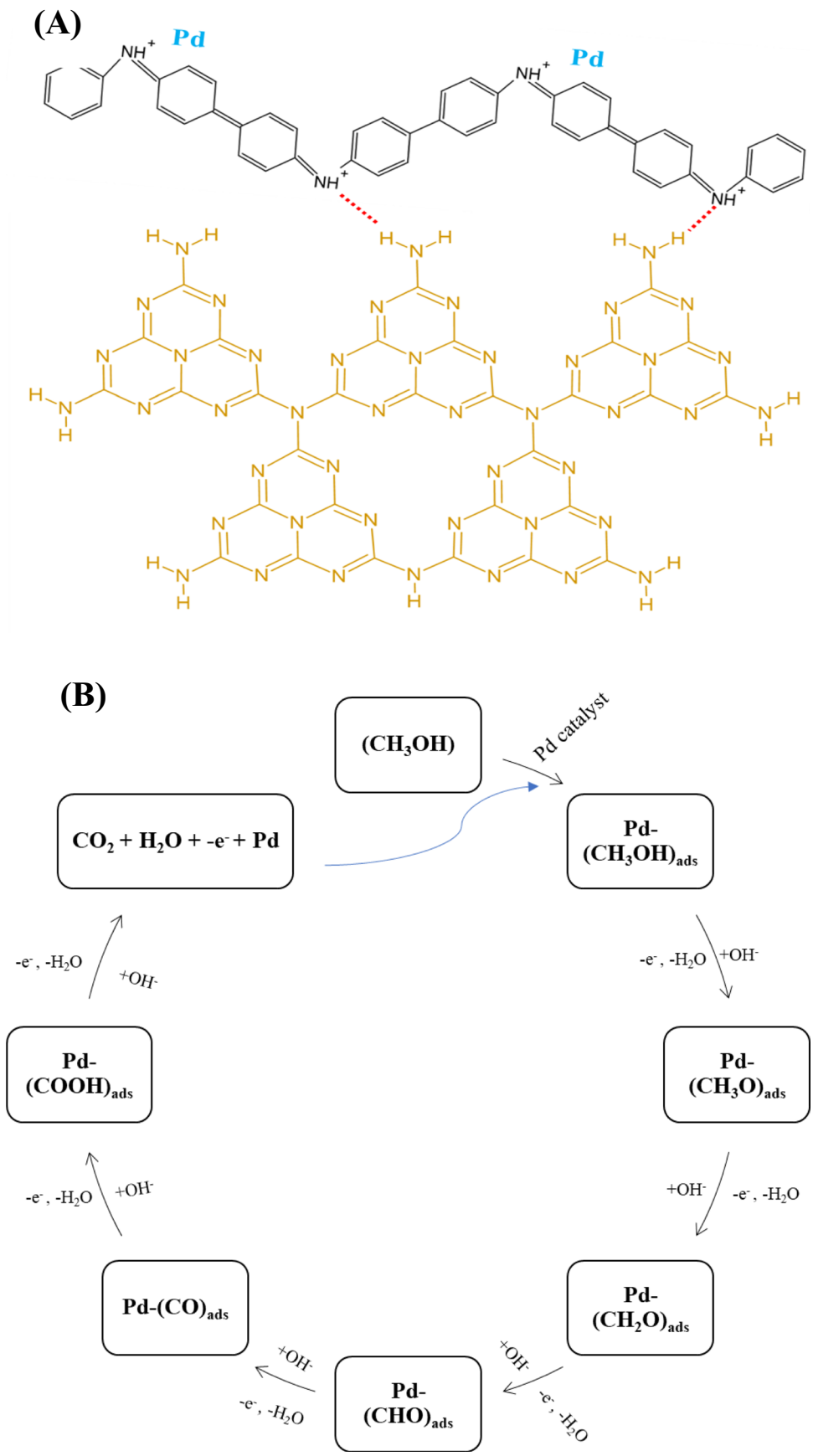

Fig. 10 (**A**) Chemical interactions of GCN/PDPA/Pd nanohybrid and (**B**) Mechanisms of GCN/PDPA/Pd nanohybrid towads MOR

The electrocatalytic activity of this catalyst was assessed for methanol electro-oxidation reaction in an alkaline medium and compared with that of commercial Pd/C catalysts through CV, CA, and EIS techniques. The GCN/PDPA/Pd NS nanohybrid electrode exhibited significant electrocatalytic activity, lower charge transfer resistance, high current density, low onset potential (− 0.15 V), and, better stability, and durability (1800s) towards MOR when compared with commercial Pd/C catalyst because of the structural morphology and electrostatic interaction of the nanohybrid materials. These findings suggest that GCN/PDPA/Pd NS nanohybrid electro-catalyst may be a good DMFC electro-catalyst for MOR in the future. Vasudevan Dhayalan thanks DST-SERB for Ramanujan Fellowship (Grant No. RJF/2020/000038).

Funding The authors would like to thank the basic research support from the National Institute of Technology Puducherry, Karaikal, India. Also, the authors are grateful to the Researchers Supporting Project Number (RSP2022R448), King Saud University, Riyadh, Saudi Arabia.

References

1. Madaswamy SL, Alothman AA, mana AL-Anazy M, Ifseisi AA, Alqahtani KN, Natarajan SK, Angaiah S, Ragupathy D (2021) Polyaniline-based nanocomposites for direct methanol fuel cells (DMFCs)-a recent review. Ind Eng Chem Res 97:79–94
2. Lakshmi MS, Wabaidur SM, Alothman ZA, Johan MR, Ponnusamy VK, Dhanusuraman R (2020) Phosphotungstic acid-Titania loaded polyaniline nanocomposite as efficient methanol electro-oxidation catalyst in fuel cells. Int J Energy Res 45:8243–8254. https://doi.org/10.1002/er.5950
3. Zhong JP, Hou C, Li L, Waqas M, Fan YJ, Shen XC, Chen W, Wan LY, Liao HG, Sun SG (2020) A novel strategy for synthesizing Fe, N, and S tridoped graphene-supported Pt nanodendrites toward highly efficient methanol oxidation. J Catal 381:275–284. https://doi.org/10.1016/j.jcat.2019.11.002
4. Keertheeswari NV, Madaswamy SL, Wabaidur SM, Habila MA, Al-Anazy MM, Dhanusuraman R, Ponnusamy VK (2021) Platinum nanoparticles/phosphotungstic acid nanorods anchored poly (diphenylamine) nanohybrid coated electrode as a superior electro-catalyst for oxidation of methanol. Prog Org Coat 161:106470. https://doi.org/10.1016/j.porgcoat.2021.106470
5. Zhang Q, Chen T, Jiang R, Jiang F (2020) Comparison of electrocatalytic activity of Pt 1–x Pd x/C catalysts for ethanol electro-oxidation in acidic and alkaline media. RSC Adv 10(17):10134–10143. https://doi.org/10.1039/d0ra00483a
6. Madaswamy SL, Wabaidur SM, Khan MR, Lee SC, Dhanusuraman R (2021) Polyaniline-graphitic carbon nitride based nano-electrocatalyst for fuel cell application: a green approach with synergistic enhanced behaviour. Macromol Res 29:411–417. https://doi.org/10.1007/s13233-021-9044-1
7. Ng JC, Tan CY, Ong BH, Matsuda A, Basirun WJ, Tan WK, Singh R, Yap BK (2019) Novel palladium-guanine-reduced graphene oxide nanocomposite as efficient electrocatalyst for methanol oxidation reaction. Mater Res Bull 112:213–220. https://doi.org/10.1016/j.materresbull.2018.12.029
8. Fang D, Yang L, Yang G, Yi G, Feng Y, Shao P, Shi H, Yu K, You D, Luo X (2020) Electrodeposited graphene hybridized graphitic carbon nitride anchoring ultrafine palladium nanoparticles for remarkable methanol electrooxidation. Int J Hydrogen Energy 45:21483–21492. https://doi.org/10.1016/j.ijhydene.2020.05.273
9. Li Z, Lin R, Liu Z, Li D, Wang H, Li Q (2016) Novel graphitic carbon nitride/graphite carbon/palladium nanocomposite as a high-performance electrocatalyst for the ethanol oxidation reaction. Electrochim Acta 191:606–615. https://doi.org/10.1016/j.electacta.2016.01.124
10. Li H, Zhang Y, Wan Q, Li Y, Yang N (2018) Expanded graphite and carbon nanotube supported palladium nanoparticles for electrocatalytic oxidation of liquid fuels. Carbon 131:111–119. https://doi.org/10.1016/j.carbon.2018.01.093
11. Murugesan B, Pandiyan N, Sonamuthu J, Samayanan S, Mahalingam S (2018) Ternary nanocomposite designed by MWCNT backbone PPy/Pd for efficient catalytic approach toward reduction and oxidation reactions. Adv Powder Technol 29:3173–3182. https://doi.org/10.1016/j.apt.2018.08.020
12. Soleimani-Lashkenari M, Rezaei S, Fallah J, Rostami H (2018) Electrocatalytic performance of Pd/PANI/TiO_2 nanocomposites for methanol electrooxidation in alkaline media. Synth Met 235:71–79. https://doi.org/10.1016/j.synthmet.2017.12.001
13. Ragupathy D, Gomathi P, Lee SC, Al-Deyab SS, Lee SH, Do Ghim H (2012) One-step synthesis of electrically conductive polyaniline nanostructures by oxidative polymerization method. J Ind Eng Chem 18:1213–1215. https://doi.org/10.1016/j.jiec.2012.01.032
14. Madaswamy SL, Keertheeswari NV, Dhanusuraman R (2022) Conducting polymers: fundamentals, synthesis, properties, and applications, 1st Edition. Conducting Polym, 29–48. CRC Press
15. Lakshmi MS, Muthusankar E, Wabaidur SM, Alothman ZA, Ponnusamy VK, Ragupathy D (2020) Development and characterization of polydiphenylamine/CuO nanohybrid electrode and its improved electrochemical properties. Sen Lett 18:5–11
16. Suba Lakshmi M, Wabaidur SM, Alothman ZA, Ragupathy D (2020) Novel 1D polyaniline nanorods for efficient electrochemical supercapacitors: a facile and green approach. Synth Met 270:116591. https://doi.org/10.1016/j.synthmet.2020.116591
17. Eswaran M, Dhanusuraman R, Tsai PC, Ponnusamy VK (2019) One-step preparation of graphitic carbon nitride/Polyaniline/Palladium nanoparticles based nanohybrid composite modified electrode for efficient methanol electro-oxidation. Fuel 251:91–97. https://doi.org/10.1016/j.fuel.2019.04.040
18. Ragupathy D, Gopalan AI, Lee KP, Manesh KM (2008) Electro-assisted fabrication of layer-by-layer assembled poly(2,5-dimethoxyaniline)/phosphotungstic acid modified electrode and electrocatalytic oxidation of ascorbic acid. Electrochem Commun 10:527–530. https://doi.org/10.1016/j.elecom.2008.01.025
19. Muthusankar E, Ragupathy D (2019) Supercapacitive retention of electrochemically active phosphotungstic acid supported poly (diphenylamine)/MnO_2 hybrid electrode. Mat Lett 241:144–147. https://doi.org/10.1016/j.matlet.2019.01.071
20. Eswaran M, Dhanusuraman R, Chokkiah C, Tsai PC, Wabaidur SM, Alothman ZA, Ponnusamy VK (2022) Poly(diphenylamine) and its nanohybrids for chemicals and biomolecules analysis: a review. Curr Anal Chem 18:546–562. https://doi.org/10.2174/1573411017999201215164018
21. Madaswamy SL, Alfakeer M, Bahajjaj AA, Ouladsmane M, Wabaidur SM, Chen CX, Dhanusuraman R (2021) Remarkable electrocatalytic activity of Pd nanoparticles dispersed on polyaniline-polydiphenylamine copolymer nanocomposite for methanol and ethanol oxidation reaction. Synthe Met 281:116925
22. Madaswamy SL, Keertheeswari NV, Alothman AA, mana AL-Anazy M, Alqahtani KN, Wabaidur SM, Dhanusuraman R (2022) Fabrication of nanocomposite networks using Pd nanoparticles/polydiphenylamine anchored on the surface of reduced graphene oxide: an efficient anode electrocatalyst for oxidation

of methanol. Adv Ind Eng Polym Res 5:18–25. https://doi.org/10.1016/j.aiepr.2021.08.001
23. Wen TC, Sivakumar C, Gopalan A (2002) Studies on processable conducting blend of poly (diphenylamine) and poly (vinylidene fluoride). Mater Lett 54:430–441. https://doi.org/10.1016/S0167-577X(01)00605-X
24. Mari E, Tsai PC, Eswaran M, Ponnusamy VK (2020) Efficient electro-catalytic oxidation of ethylene glycol using flower-like graphitic carbon nitride/iron oxide/palladium nanocomposite for fuel cell application. Fuel 280:118646. https://doi.org/10.1016/j.fuel.2020.118646
25. Pieta IS, Rathi A, Pieta P, Nowakowski R, Hołdynski M, Pisarek M, Kaminska A, Gawande MB, Zboril R (2019) Electrocatalytic methanol oxidation over Cu, Ni and bimetallic Cu-Ni nanoparticles supported on graphitic carbon nitride. Appl Catal B Environ 244:272–283. https://doi.org/10.1016/j.apcatb.2018.10.072
26. Li CZ, Wang ZB, Sui XL, Zhang LM, Gu DM (2015) Ultrathin graphitic carbon nitride nanosheets and graphene composite material as high-performance PtRu catalyst support for methanol electro-oxidation. Carbon 93:105–115. https://doi.org/10.1016/j.carbon.2015.05.034
27. Zhang W, Huang H, Li F, Deng K, Wang X (2014) Palladium nanoparticles supported on graphitic carbon nitride-modified reduced graphene oxide as highly efficient catalysts for formic acid and methanol electrooxidation. J Mater Chem A 2:19084–19094. https://doi.org/10.1039/c4ta03326d
28. Qian H, Huang H, Wang X (2015) Design and synthesis of palladium/graphitic carbon nitride/carbon black hybrids as high-performance catalysts for formic acid and methanol electrooxidation. J Power Sources 275:734–741. https://doi.org/10.1016/j.jpowsour.2014.10.109
29. Qian H, Chen S, Fu Y, Wang X (2015) Platinum-palladium bimetallic nanoparticles on graphitic carbon nitride modified carbon black: a highly electroactive and durable catalyst for electrooxidation of alcohols. J Power Sources 300:41–48. https://doi.org/10.1016/j.jpowsour.2015.09.051
30. Bhowmik T, Kundu MK, Barman S (2017) Highly efficient electrocatalytic oxidation of formic acid on palladium nanoparticles-graphitic carbon nitride composite. Int J Hydrogen Energy 42:212–217. https://doi.org/10.1016/j.ijhydene.2016.11.095
31. Fan JJ, Fan YJ, Wang RX, Xiang S, Tang HG, Sun SG (2017) A novel strategy for the synthesis of sulfur-doped carbon nanotubes as a highly efficient Pt catalyst support toward the methanol oxidation reaction. J of Mater Chem A 5(36):19467–19475. https://doi.org/10.1039/C7TA05102F
32. Wang RX, Fan YJ, Wang L, Wu LN, Sun SN, Sun SG (2015) Pt nanocatalysts on a polyindole-functionalized carbon nanotube composite with high performance for methanol electrooxidation. J Power Sources 287:341–348. https://doi.org/10.1016/j.jpowsour.2015.03.181
33. Xiang S, Wang L, Huang CC, Fan YJ, Tang HG, Wei L, Sun SG (2018) Concave cubic PtLa alloy nanocrystals with high-index facets: controllable synthesis in deep eutectic solvents and their superior electrocatalytic properties for ethanol oxidation. J Power Sources 399:422–428. https://doi.org/10.1016/j.jpowsour.2018.07.102
34. Zhang JM, Sun SN, Li Y, Zhang XJ, Zhang PY, Fan YJ (2017) A strategy in deep eutectic solvents for carbon nanotube-supported PtCo nanocatalysts with enhanced performance toward methanol electrooxidation. Int J Hydrog Energy 43:26744–26751. https://doi.org/10.1016/j.ijhydene.2017.09.090
35. Liu F, Yang X, Dang D, Tian X (2019) Engineering of hierarchical and three-dimensional architectures constructed by titanium nitride nanowire assemblies for efficient electrocatalysis. Chem ElectroChem 8:2208–2214. https://doi.org/10.1002/celc.201900252
36. Tian H, Yu Y, Wang Q, Li J, Rao P, Li R, Du Y, Jia C, Luo J, Deng P, Shen Y (2021) Recent advances in two-dimensional Pt based electrocatalysts for methanol oxidation reaction. Int J Hydrog Energy 61:31202–31215. https://doi.org/10.1016/j.ijhydene.2021.07.006
37. Tian H, Wu D, Li J, Luo J, Jia C, Liu Z, Huang W, Chen Q, Shim CM, Deng P, Shen Y (2022) Rational design ternary platinum based electrocatalysts for effective methanol oxidation reaction. J Energy Chem 70:230–235. https://doi.org/10.1016/j.jechem.2022.02.021
38. Raveendran A, Chandran M, Wabaidur SM, Islam MA, Dhanusuraman R, Ponnusamy VK (2022) Facile electrochemical fabrication of nickel-coated polydiphenylamine (Ni/PDPA) nanocomposite material as efficient anode catalyst for direct alcohol fuel cell application. Fuel 15(324):124424. https://doi.org/10.1016/j.fuel.2022.124424